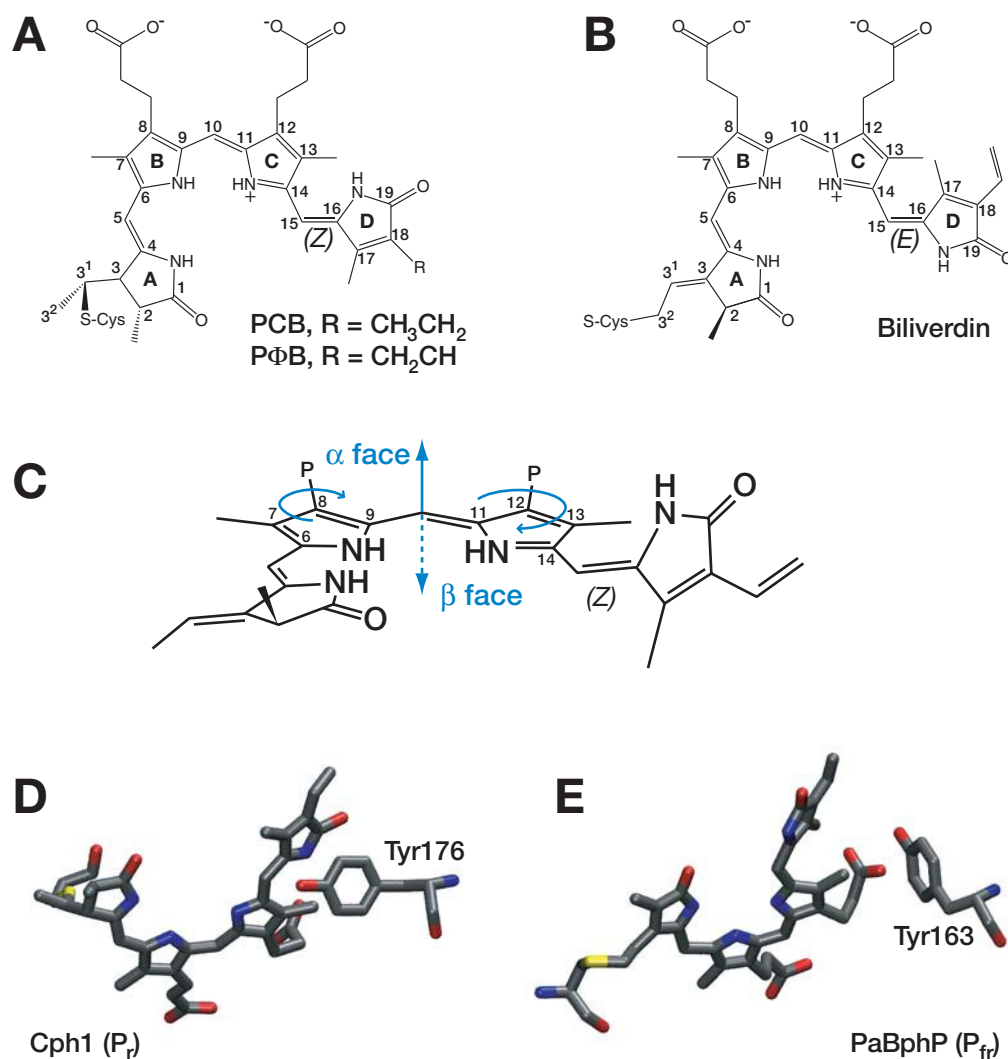


# Supporting Information

Rockwell et al. 10.1073/pnas.0902370106



**Fig. S1.** Structure and nomenclature of bilin chromophores. (A) The structure of the phytobilins phycocyanobilin (PCB) and phytochromobilin (PΦB) is shown in the C5-*Z*,*syn* C10-*Z*,*syn* C15-*Z*,*anti* configuration of Cph1 in the P<sub>r</sub> state. Ring names and numbering are shown, as is the *Z* configuration of the 15,16 double bond. (B) The structure of biliverdin IX $\alpha$  (BV) is shown in the C5-*Z*,*syn* C10-*Z*,*syn* C15-*E*,*anti* configuration of PaBphP in the P<sub>fr</sub> state. Stereochemistry at C2 is inferred from that observed in the high-resolution structure of DrBphP in the P<sub>r</sub> state. (C) The convention for naming bilin facial dispositions is shown for the BV chromophore of DrBphP in the P<sub>r</sub> state. The P<sub>r</sub> D-ring lies on the  $\alpha$  face of the coplanar B- and C-rings. Views in A and B are thus from the  $\alpha$  face. (D) The locations of PCB and Tyr-176 in the crystal structure of the Cph1 P<sub>r</sub> state (Protein Data Bank ID code 2VEA) are shown from the  $\beta$ -face. (E) A similar view is shown for BV and Tyr-163 in the crystal structure of the PaBphP P<sub>fr</sub> state (Protein Data Bank ID code 3C2W).

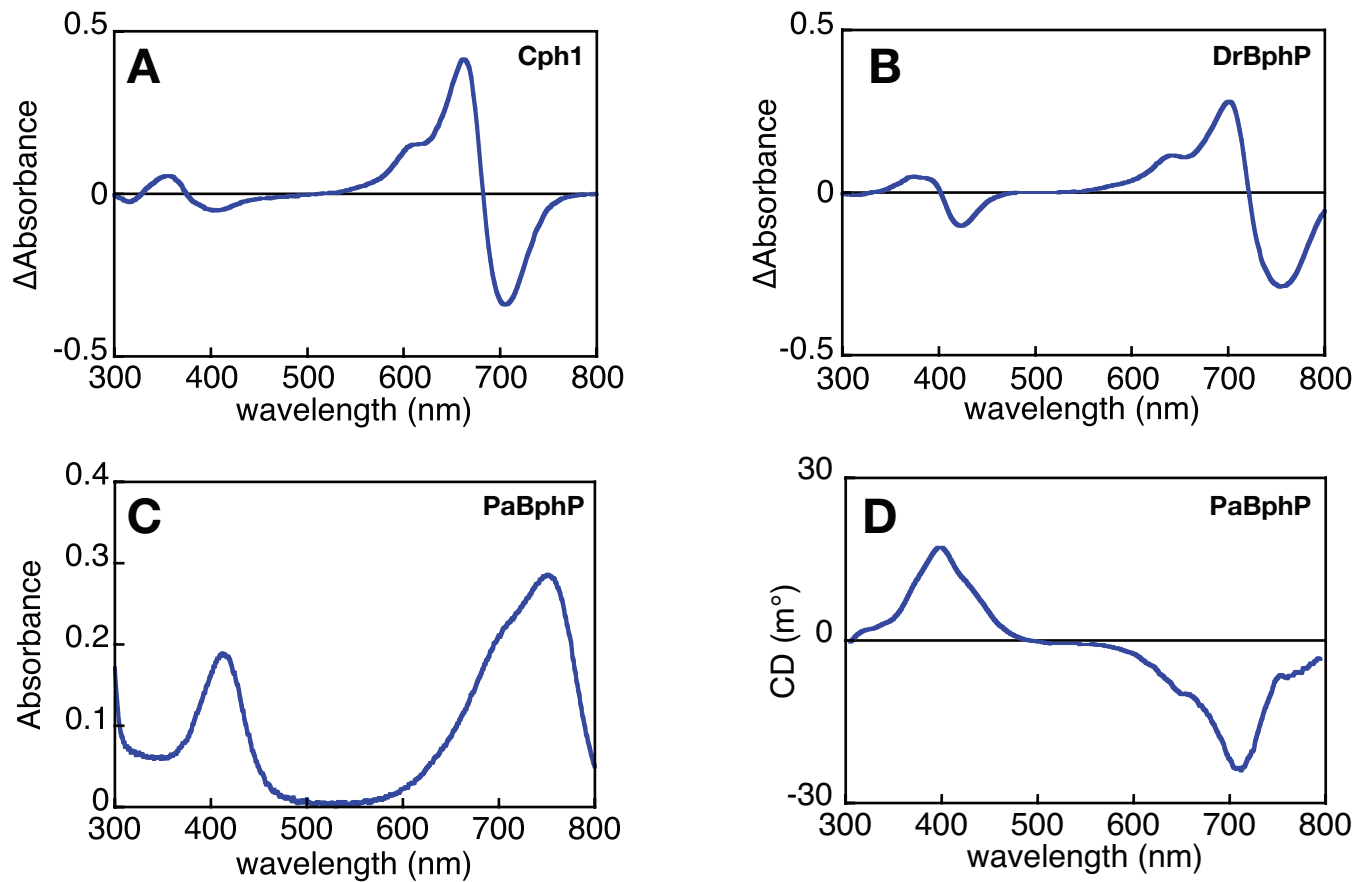
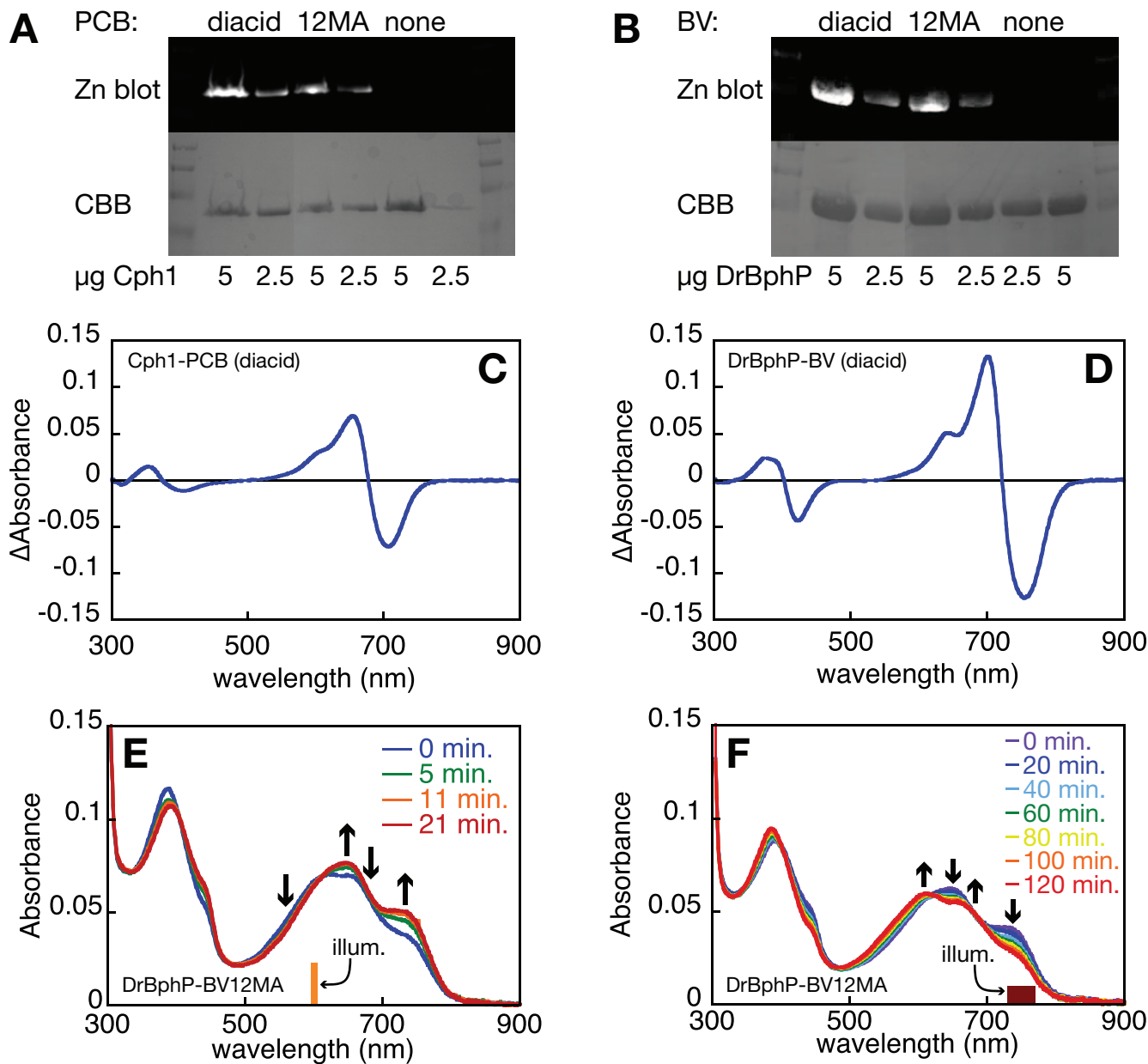
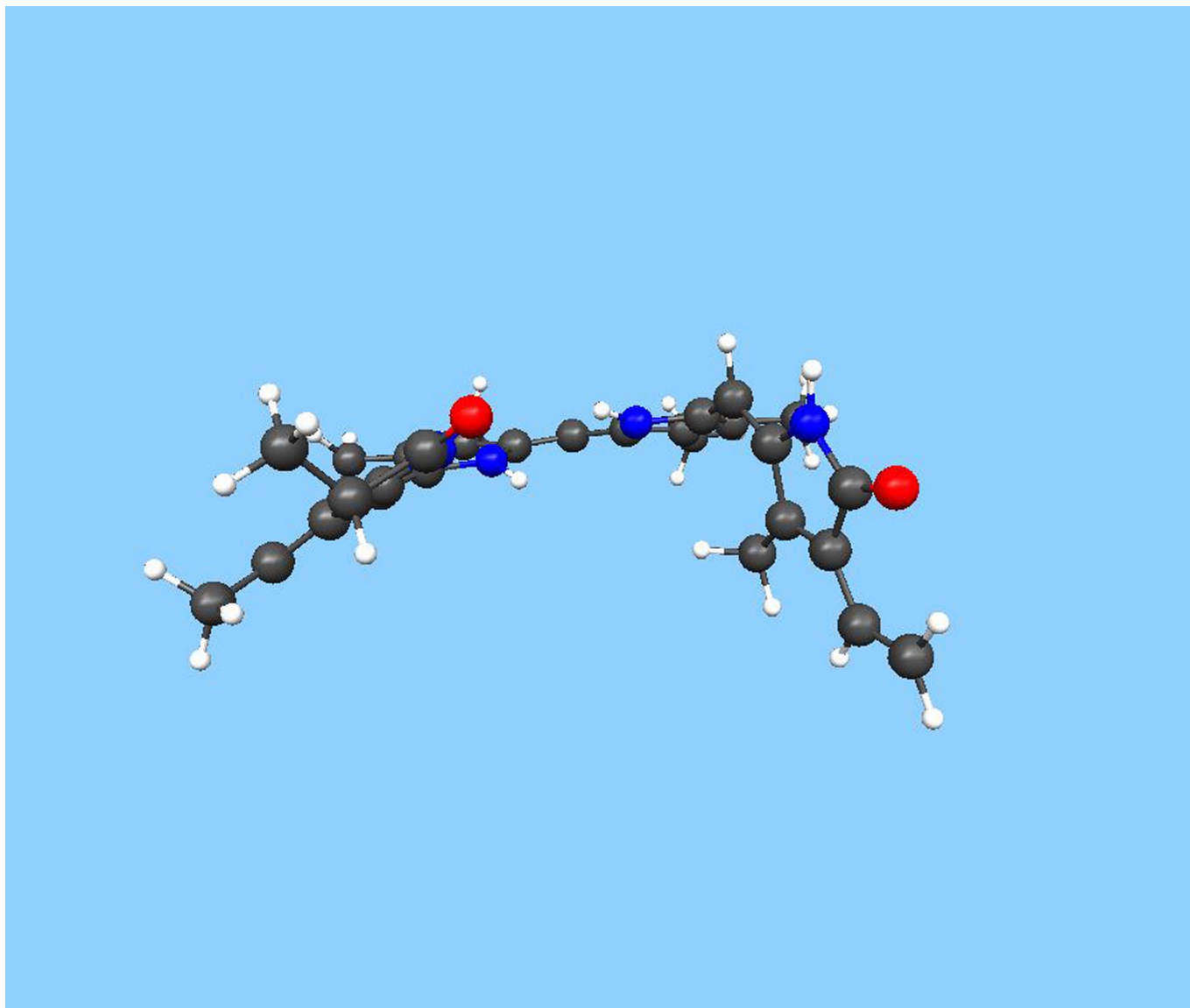


Fig. S2. Spectroscopic characterization of Cph1, DrBphP, and PaBphP. (A) The photochemical difference spectrum is shown for Cph1. (B) The photochemical difference spectrum is shown for DrBphP. (C) The absorbance spectrum of the thermally-stable  $P_r/P_{fr}$  equilibrium state of PaBphP is shown. (D) The CD spectrum of PaBphP is shown.

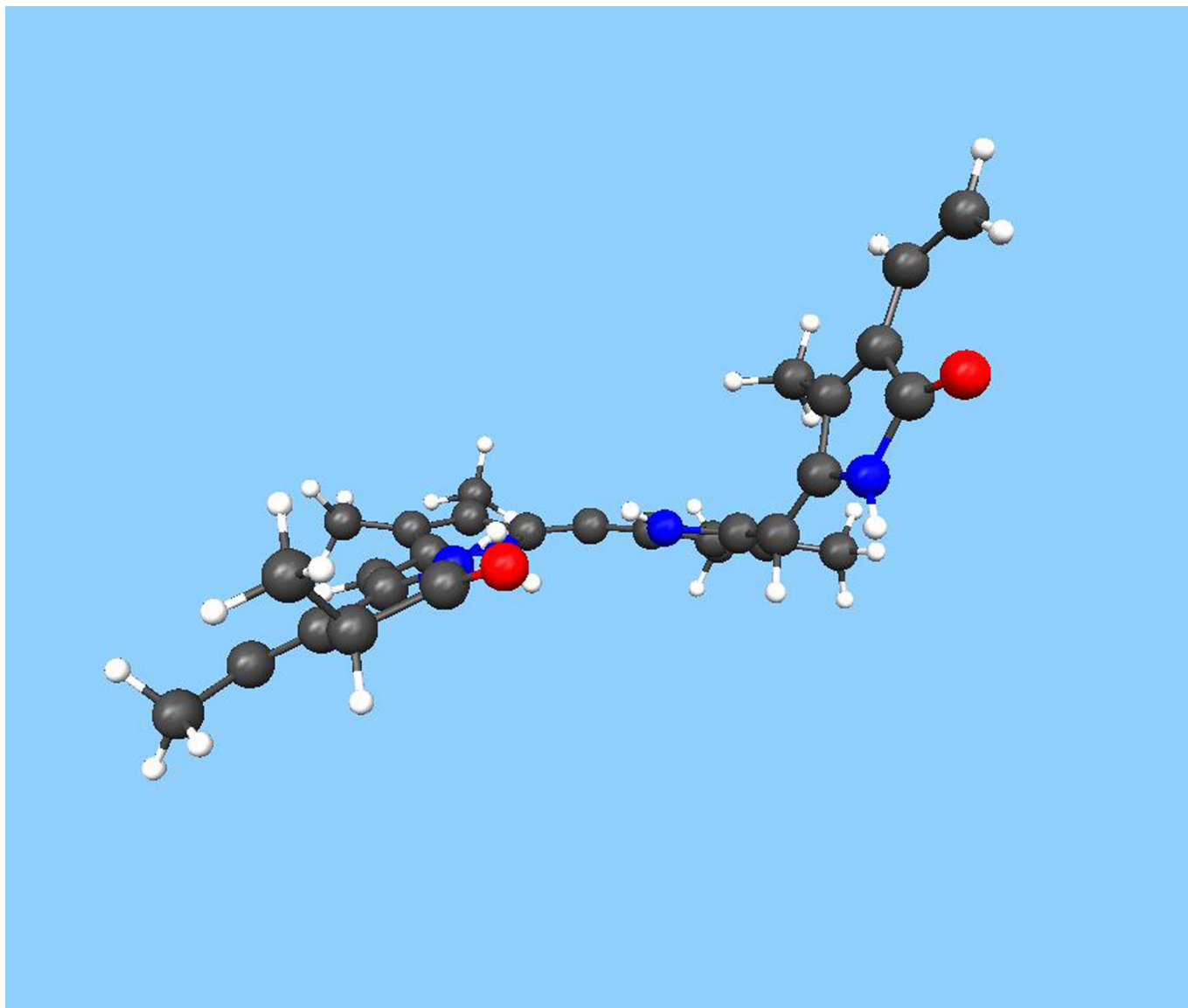


**Fig. S3.** Characterization of phytochromes assembled with chromophore 12-monoamides. (A) ApoCph1 was incubated with PCB, PCB 12-monoamide (PCB12MA), or a solvent control (DMSO) for 2 h and then subjected to overnight dialysis to remove unbound chromophore. The resulting preparations were characterized by SDS/PAGE and zinc blotting to confirm the presence of covalently-bound chromophore. (B) ApoDrBphP was similarly incubated and analyzed. (C) The photochemical difference spectrum is shown for Cph1 after assembly with PCB. (D) The photochemical difference spectrum is shown for DrBphP after assembly with BV. (E) The covalent adduct of DrBphP with BV12MA (DrBphP-BV12MA) was illuminated with  $600 \pm 5$  nm light for the indicated times, and conversion of both dual- $P_r$  peaks to both dual- $P_{fr}$  peaks was observed. (F) The photoequilibrium mixture, generated by 600 nm illumination (E), was then irradiated with  $750 \pm 20$  nm light for the indicated times to examine regeneration of dual- $P_r$ .



**Movie S1.** A model compound mimicking the  $P_r$  chromophore of *DrBphP* was manually rotated counterclockwise about the 15/16 bond to give a formally C15-*E,anti* geometry. The resulting geometry was then optimized and animated as described in *Materials and Methods*. Initial counterclockwise rotation results in movement of the D-ring to the bilin  $\beta$ -face.

[Movie S1 \(MOV\)](#)



**Movie S2.** A model compound mimicking the P<sub>1</sub> chromophore of DrBphP was manually rotated clockwise about the 15/16 bond to give a formally C15-*E,anti* geometry. The resulting geometry was then optimized and animated as described in *Materials and Methods*. Initial clockwise rotation results in retention of the D-ring on the bilin  $\alpha$ -face.

[Movie S2 \(MOV\)](#)

